

Document downloaded from:

<http://hdl.handle.net/10251/104451>

This paper must be cited as:

Traffano-Schiffo, MV.; Laghi, L.; Castro Giraldez, M.; Tylewicz, U.; Romani, S.; Ragni, L.; Dalla Rosa, M.... (2017). Osmotic dehydration of organic kiwifruit pre-treated by pulsed electric fields: Internal transport and transformations analyzed by NMR. *Innovative Food Science & Emerging Technologies*. 41:259-266. doi:10.1016/j.ifset.2017.03.012



The final publication is available at

<http://dx.doi.org/10.1016/j.ifset.2017.03.012>

Copyright Elsevier

Additional Information

Manuscript Details

Manuscript number	IFSET_2017_170
Title	OSMOTIC DEHYDRATION OF ORGANIC KIWIFRUIT PRE-TREATED BY PULSED ELECTRIC FIELDS INTERNAL TRANSPORT AND TRANSFORMATIONS ANALIZED BY NMR
Article type	Research Paper

Abstract

This work analyze the effect of Pulsed Electric Fields (PEF) as a pre-treatment of the osmotic dehydration (OD) of kiwifruit (*Actinidia deliciosa* cv Hayward) in the internal structure and in the internal water transport. PEF pre-treatments were done using three PEF intensities (100, 250 and 400 V/cm) and analyzed by TD-NMR. The OD was carried out by immersing the samples in 61.5% sucrose solution at 25 °C. The application of a PEF pre-treatment before the OD produces a process of plasmolysis proportional to the electric field applied. It is because the PEF remove the mobile charges of the medium, such as electrolytes, organic acids, aminoacids; Ca⁺² is the major culprit of the plasmolysis because it fixes some of the junctions of the microtubules between the cell wall and the membrane. Therefore, a previous plasmolysis produces an increase in the apoplasmic transport increasing the rate of dehydration.

Keywords Kiwifruit, Pulsed Electric Fields, Osmotic dehydration, TD-NMR, Water distribution, Plasmolysis.

Corresponding Author Pedro J. Fito

Corresponding Author's Institution Universitat Politecnica de Valencia

Order of Authors Maria Victoria Traffano-Schiffo, Luca Laghi, Marta Castro-Giraldez, Urszula Tylewicz, Santina Romani, Luigi Ragni, marco DALLA ROSA, Pedro J. Fito

Submission Files Included in this PDF

File Name [File Type]

Cover letter kiwi NMR 2.docx [Cover Letter]

Revisiones.docx [Response to Reviewers]

maintext KIWI NMR 2 rev 200317.docx [Manuscript File]

Figure 1.pdf [Figure]

Figure 2.pdf [Figure]

Figure 3.pdf [Figure]

Figure 4.pdf [Figure]

Figure 5.pdf [Figure]

Table 1.docx [Table]

Table 2.docx [Table]

Highlights.docx [Highlights]

Industrial relevance.docx [Highlights]

FIGURE CAPTIONS.docx [Supporting File]

To view all the submission files, including those not included in the PDF, click on the manuscript title on your EVISE Homepage, then click 'Download zip file'.

1 **OSMOTIC DEHYDRATION OF ORGANIC KIWIFRUIT PRE-TREATED BY**
2 **PULSED ELECTRIC FIELDS: INTERNAL TRANSPORT AND**
3 **TRANSFORMATIONS ANALIZED BY NMR**

4 **Maria Victoria Traffano-Schiffo^a, Luca Laghi^{b,c}, Marta Castro-Giraldez^a,**
5 **Urszula Tylewicz^b, Santina Romani^{b,c}, Luigi Ragni^{b,c}, Marco Dalla Rosa^{b,c}, Pedro**
6 **J. Fito^{a*}**

7 ^a Instituto Universitario de Ingeniería de Alimentos para el Desarrollo, Universitat
8 Politecnica de Valencia, Camino de Vera s/n, 46022 Valencia, Spain

9 ^b Department of Agricultural and Food Sciences, University of Bologna, Piazza
10 Goidanich 60, 47521 Cesena, Italy

11 ^c Interdepartmental Centre for Agri-Food Industrial Research, University of Bologna,
12 Via Quinto Bucci 336, 47521 Cesena, Italy

13 *author for correspondence: pedfisu@tal.upv.es

14

15 **ABSTRACT**

16 This work analyzes the effect of Pulsed Electric Fields (PEF) as a pre-treatment of the
17 osmotic dehydration (OD) of kiwifruit (*Actinidia deliciosa* cv *Hayward*) in the internal
18 structure and in the internal water transport. PEF pre-treatments were done using three
19 PEF intensities (100, 250 and 400 V/cm) and analyzed by TD-NMR. The OD was
20 carried out by immersing the samples in 61.5% sucrose solution at 25 °C. The
21 application of a PEF pre-treatment before the OD produces a process of plasmolysis
22 proportional to the electric field applied. It is because the PEF removes the mobile
23 charges of the medium, such as electrolytes, organic acids, aminoacids; Ca⁺² is the

24 major culprit of the plasmolysis because it fixes some of the junctions of the
25 microtubules between the cell wall and the membrane. Therefore, a previous
26 plasmolysis produces an increase in the apoplastic transport increasing the rate of
27 dehydration.

28

29 Keywords: Kiwifruit, Pulsed Electric Fields, Osmotic dehydration, TD-NMR, Water
30 distribution, Plasmolysis.

31

32 **NOTATION**

33 x_i mass fraction of i chemical specie ($\text{kg}_i \text{kg}_T^{-1}$)

34 T_2 spin-spin or proton transverse relaxation time

35 r_I relative intensities

36 M mass (kg)

37 S surface of samples (m^2)

38 r radius (m)

39 X_{w0}^{ADS} monomolecular moisture layer ($\text{kg}_w \text{kg}_{\text{dm}}^{-1}$)

40 N_A avogadro number ($6.022 \cdot 10^{23}$ molecules mol^{-1})

41 M_w molecular weight of water (18 g mol^{-1})

42 t treatment time

43 I Intensity

44 E electric field (V cm^{-1})

45

46 *Subscripts*

47 w water

48	T	total
49	0	raw sample
50	1	sample after the pre-treatment by PEF
51	i	internal
52	j	any chemical species
53	<i>Superscripts</i>	
54	j	specific group of water molecules j
55	t	treatment time (s)
56	0	initial time
57	ELP	extracellular liquid phase
58	ILP	intracellular liquid phase
59	ADS	adsorbed water

60 **1. Introduction**

61 Cellular structure is considered as a complex organized system where flows are carried
62 out by different solutes or solvents transports systems. Based on the free energy
63 gradients, commonly known as passive transports, symplastic, aploplastic and
64 aquaporins transmembrane transports are involved. Firstly, cells are interconnected by
65 plasmodesmatas which led to generate symplastic transports across them. In the
66 extracellular space, the fluxes are produced by apoplastic pathways (Marcotte, Toupin,
67 & Le Maguer, 1991) and finally, the transmembrane transport is characterized by the
68 exchange between intra and extracellular spaces by protein channels, called aquaporins
69 (Agre et al., 2002; Maurel & Chrispeels, 2001). In contrast, when the flows occur in
70 the opposite direction of the free energy gradients, they are produced by protein
71 channels and they require energy consumption as adenosine triphosphate (ATP)
72 (Moraga, Moraga, Fito, & Martínez-Navarrete, 2009). The main active pumps are
73 Ca^{2+} , Na^{+} and $\text{Na}^{+}/\text{K}^{+}$, which are the responsible of the transport of water, sucrose and
74 electrolytes (Traffano-Schiffo et al., 2016).

75 Taking into account the water content, Tylewicz, Fito, Castro-Giráldez, Fito, & Dalla
76 Rosa (2011) explain that the water distribution in fresh kiwifruit can be segregated in
77 adsorbed water (solid matrix) and liquid water. In turn, for parenchymatic tissue, the
78 liquid water can be divided into intra and extracellular liquid phases. During osmotic
79 dehydration (OD) treatment, the water distribution of the cellular structure changes
80 due to mass transfer phenomena, which are generated as a consequence of the water
81 and sucrose chemical differences between the tissue and the osmotic solution
82 (Traffano-Schiffo et al., 2016; Khin, Zhou, & Perera, 2006, Castro-Giráldez,
83 Tylewicz, Fito, Dalla Rosa, & Fito, 2011; Castro-Giráldez, Fito, Dalla Rosa, & Fito,

84 2011). From the contact of the fruit tissue with the osmotic solution, the
85 semipermeable membranes, plasma membrane and the tonoplast are forced to separate,
86 due to the water losses from the vacuoles, starting the process known as plasmolysis,
87 characterized by the loss of the turgor pressure (Lang, Sassmann, Schmidt, & Komis,
88 2014; Lang, Barton, & Overall, 2004). Plasmolysis occurs in two stages: partial and
89 the complete plasmolysis. Partial plasmolysis is produced when the plasma membrane
90 starts to detach from the cell wall and the complete plasmolysis occurs when the
91 complete separation of the protoplast is produced (Seguí, Fito, & Fito, 2012).

92 For many years, OD has been extensively studied around the world for the partial
93 dehydration of fruits and vegetables; however, it presents some limitations such as the
94 low dehydration rate and the high solute content in the final product. Therefore, the
95 use of pre-treatment such as Pulsed Electric Fields (PEF) has been reported to facilitate
96 water removal and to improve the quality of the dried products (Dermesonlouoglou,
97 Zachariou, Andreou, & Taoukis, 2016; Dellarosa et al., 2016; Barba et al., 2015).

98 PEF is a non-thermal technology which involves the application of short and repeated
99 voltage pulses to a biological tissue placed between two electrodes (Gürsul, Gueven,
100 Grohmann, & Knorr, 2016); it induces changes and reorganization in the electric
101 conformation of the cell membrane (Baier, Bußler, & Knorr, 2015), modifying the
102 normal fluxes during drying process when it is used as a pre-treatment.

103 Time Domain Nuclear Magnetic Resonance (TD-NMR) is a non-destructive technique
104 able to determine the spin-spin or transverse relaxation (T_2) of protons and the intensity
105 of the signal, differentiating extracellular space, vacuoles and solid matrix
106 (Santagapita et al., 2013). TD-NMR is considered as one of the most powerful

107 techniques able to follow the water distribution in cellular tissues, thus, it is necessary
108 for describe the driving forces that promote the water fluxes.

109 The aim of this research was to determine the effect of PEF pre-treatment in the
110 microstructure and in the internal water transport throughout an osmotic treatment of
111 kiwifruit in hypertonic sucrose solution.

112

113 2. Material and methods

114 Organic kiwifruits (*Actinidia deliciosa* cv “Hayward”) with the same ripeness and
115 similar size were bought on a supermarket located in Cesena (Italy) and kept
116 refrigerated at 4 ± 1 °C until use. The fruits were tempered at 25 °C, peeled and
117 cylinders (8 mm diameter and 10 mm length) were obtained from the outer pericarp,
118 avoiding the core, the inner pericarp and the seeds. The initial solute content of the
119 fruits used were 13 ± 1 ° Brix.

120 Fresh kiwifruits were characterized by mass, volume, solutes (° Brix), water activity
121 (a_w), moisture (x_w) and TD-NMR by quadruplicate. 12 sample cylinders were used for
122 each treatment (total number of treated samples of 576). They were placed inside the
123 PEF chamber avoiding free spaces between them and subjected to different electric
124 fields strengths. Immediately after, the samples were weighed and introduced into the
125 osmotic dehydration solution. According to previous results, the selected OD
126 treatment times were 0, 10, 20, 30, 60 and 120 min (Traffano-Schiffo et al., 2016).

127 Due to the fact that the samples after treatments show concentration profiles, another
128 batch of samples were treated and equilibrated at 4 °C during 24 hours in decagon
129 containers closed with parafilm®. Finally, mass, volume, solute content (° Brix), a_w , x_w
130 and TD-NMR were measured as final determinations for treated and equilibrated

131 samples. In addition, at each osmotic time, an aliquot of sucrose solution was taken to
132 measure a_w and solute content.

133

134 **2.1. PEF treatment**

135 Pulsed electric field treatments were applied to the samples using monopolar pulse
136 generator equipment based on MOSFET technology and capacitors as energy tanks
137 (Dellarosa et al., 2016). The cylinders of organic kiwifruit were placed in a rectangular
138 treatment chamber avoiding free spaces between them. The chamber was equipped
139 with two stainless steel electrodes (20 x 20 mm²) with a separation between them of
140 30 mm and filled with 5 mL of tap water with an electrical conductivity of 328 ± 4
141 $\mu\text{S/cm}$ at 25 °C.

142 PEF pre-treatments were done by applying three different pulsed electric fields (100,
143 250 and 400 V/cm at 50 Hz) with near-rectangular shape pulses, a train of 60 pulses,
144 a fixed pulse width of $100 \pm 2 \mu\text{s}$ and a repetition time of $10.0 \pm 0.1 \text{ ms}$.

145

146 **2.2. Osmotic dehydration treatment**

147 The osmotic solution at 61.5% (w/w) was prepared with commercial sucrose and
148 distilled water at 25 °C. Samples were immersed into the sucrose solution maintaining
149 a relationship of 1:4 (w/w) between the fruit and the solution.

150

151 **2.3. Analytical determinations**

152 A dew point Hygrometer Decagon (Aqualab™, series 3 TE) was used for measuring
153 the water activity, with a precision ± 0.003 . Mass was determined by using a Kern
154 balance ABS 320-4N (± 0.0001) (KERN & SOHN GmbH, Germany).

155 The analysis of the moisture was accomplished following the AOAC Method 934.06,
156 2000.

157 Sugar content was determined by measuring the refractometric index with a digital
158 refractometer (KRÜSS Optronic[©] GmbH, Germany) calibrated with distilled water at
159 25 °C. The sample was pressed in order to extract the external liquid phase. Solute
160 content was measured by refractometry of both kiwifruit samples and osmotic solution
161 after the treatments.

162 Analytical determinations described above were obtained by quadruplicate.

163

164 **2.4. TD-NMR measurements**

165 Proton transverse relaxation time (T_2) decay was measured for each sample by
166 applying the CPMG pulse sequence (Meiboom & Gill, 1958), using a Bruker ‘The
167 Minispec’ spectrometer (Bruker Corporation, Germany) operating at 20 MHz, as
168 described by Dellarosa et al. (2016). Each measurement comprised 32000 echoes, with
169 an interpulse spacing of 0.08 ms and a recycle delay of 10 s, which allowed the
170 measurement of proton decays included between 1 and 3000 ms and avoided sample
171 overheat. Each acquisition was performed over 8 scans giving rise to a total time of
172 analysis around 90 s. The registered spectra were normalized to unitary area and
173 analyzed by UpenWin software (Borgia, Brown, & Fantazzini, 1998) to give quasi-
174 continuous distributions of relaxation time. The number of output relaxation times,
175 sampled logarithmically in the 1–3000 ms range, was set to 100. To obtain quantitative
176 information from the T_2 -weighted decay curves, signals were fitted using a discrete
177 multi-exponential curve. The fitting was run using the ‘Levenberg–Marquardt
178 nonlinear least squares’ algorithm implemented in ‘R’ software (R Foundation for

179 Statistical Computing, Austria). Unlike Santagapita et al. (2013), the optimum number
180 of exponential curves for each tested treatment was found to be three, without
181 removing any initial T_2 weighted point.

182

183 **2.5. Low-temperature scanning electron microscopy (Cryo-SEM)**

184 Microstructure was analyzed by Cryo-SEM. A Cryostage CT-1500C unit (Oxford
185 Instruments, Witney, UK), coupled to a Jeol JSM-5410 scanning electron microscope
186 (Jeol, Tokyo, Japan). The sample was immersed in N_2 slush ($-210\text{ }^\circ\text{C}$) and then quickly
187 transferred to the Cryostage at 1 kPa where sample fracture took place. Sublimation
188 (etching) was carried out at $-95\text{ }^\circ\text{C}$. The final point was determined by direct
189 observation under the microscope, working at 5 kV. Then, once again in the Cryostage
190 unit, the sample was coated with gold in vacuum (0.2 kPa) applied for 3 min, with an
191 ionization current of 2 mA. The observation in the scanning electron microscope was
192 carried out at 20 kV, at a working distance of 15 mm and temperature $\leq -130\text{ }^\circ\text{C}$.

193

194 **3. Results and discussion**

195 Fruit tissue, such as kiwifruit, is composed by parenchymatic and vascular tissues,
196 where cells with big vacuoles coexist with vascular cells. This system is full of
197 chemical species charged, with capacity to orientate and move with an external electric
198 field. Moreover, these compounds, with high electric activity, are responsible of part
199 of the cell pathways and metabolisms. Therefore, any electric disturb in the fruit tissue
200 produces high disorder in the cell functionality. Moreover, biological cells are
201 delimited by a phospholipid bilayer membrane (protoplast and tonoplast), which
202 separates the internal liquid phase from a completely different external medium.

203 Despite there is an electric equilibrium at both sides of the bilayer, the concentration
204 and nature of the charged compounds are different (Bezanilla, 2008). When a
205 biological tissue is subjected to an external electric field, it induces changes in the
206 electric conformation of the bilayer and in the involved chemical species (Traffano-
207 Schiffo et al., 2016). Therefore, the different liquid mediums and the solid matrix
208 suffer transformations with the application of external electric fields.

209 Table 1 shows the main chemical species of kiwifruit with capability to orientate and
210 migrate when an external electric field at low frequency is applied. These species are:
211 electrolytes with biological activity, responsible of the active transport pumps and
212 bonds of the middle lamella; aminoacids, part of proteins channels or passive transport
213 pumps; chlorophylls, carotenoids and anthocyanins, greatly charged antioxidant
214 compounds with functional activity and organic acids, which regulate de pH of the
215 fruit and play an important role in the respiration pathway. These quantities of different
216 chemical species, with different electric nature, shows the complexity in the
217 explanation of the effects in the kiwifruit tissue affected by an external electric field.

218

219 In order to understand the correct functionality of the biological tissue under the effect
220 of an external electric field, it is necessary to know the involved metabolic transports.
221 Figure 1a shows a schematic representation of the cellular transports. Inside the
222 cellular tissue, fluxes occur by different pathways: apoplastic, symplastic and
223 transmembrane (aquaporins) transports or passive transports, produced by free energy
224 gradients and the transmembrane transport or active transport, which is based on
225 proteins channels and with ATP consumption (Johansson, Karlsson, Johanson,
226 Larsson, & Kjellbom, 2000). Previously, it has been demonstrated that the application

227 of an external electric field through the vegetal tissue induces compositional changes
228 (removing part of the native electrolytes such as Ca^{2+} and Na^+) and, as a consequence,
229 the transmembrane active transports are affected. The main affected transmembrane
230 active transports are: Ca^{2+} pump which is the responsible to maintain the homeostatic
231 cellular system (water transport) and Na^+ pump, responsible of sucrose transmembrane
232 transport (Traffano-Schiffo et al., 2016).

233

234 Figure 1a shows the schematic diagram of a plant cell tissue where it is possible to
235 observe the different active and passive transports that can be produced. These
236 transports are classified by the extracellular transport (apoplastic), the transport
237 between cells or intracellular (symplastic) and the transmembrane that communicates
238 both phases. These spaces are described by their corresponding liquid phases,
239 extracellular (ELP) and intracellular (ILP). Figure 1b shows two micrographs obtained
240 by Cryo-SEM, the upper picture shows raw parenchyma tissue of kiwifruit and the
241 lower one shows partially dehydrated parenchymal tissue with symptoms of
242 plasmolysis.

243 Figure 1c shows examples of the distribution of T_2 -weighted signals obtained by TD-
244 NMR in parenchyma tissue of kiwifruit in the present research. The three protons
245 populations that were observed in the non pre-treated samples had T_2 or relaxation
246 times of 1170, 425 and 53. The smaller the T_2 , the lower the mobility of the molecule
247 with the induced proton is, so that it is possible to determine the origin of each group
248 of molecules in function of the different motion capacity of water molecules in the
249 tissue. The lower value of T_2 corresponds to water molecules with less mobility, water
250 molecules subjected to electrical adsorption forces. This group is adsorbed on the cell

251 wall and on the cell membrane (protoplast and tonoplast), thus it can be considered the
252 entire adsorbed water of tissue. The remaining groups might correspond to the
253 different liquid phases that make up the parenchyma, from the interior of the cell
254 mostly occupied by the vacuole (higher T_2 and higher intensity), named ILP, and
255 external liquid phase (intermediate T_2), named ELP. Therefore, the intensities
256 measured in NMR, can be divided in three groups of water molecules; Adsorbed, ELP
257 and ILP. They are shown in Table 2.

258

259 As previously described by different authors (Nakashima, 2001; Muller, Scrivener,
260 Gajewicz, & McDonald, 2013; Traffano-Schiffo et al., 2017), it is possible to divide
261 the water molecules into groups according to their situation in the tissue using a value
262 of proportionality to the intensity measured by NMR as it is shown in Table 2. The
263 relative intensities (r_I^j) of a specific group of water molecules (j) along OD treatment
264 can be defined as the relationship between the intensity of each group of water
265 molecules and the overall measured intensity. This parameter let to obtain the water
266 distribution (x_w^j) of a specific group of water molecules (j) as follows:

$$267 \quad x_w^j = x_w \cdot r_I^j \quad (1)$$

268 Where x_w^j is the water mass fraction of water group j ($\text{kg}_{w \text{ in } j}/\text{kg}_T$) and x_w is the water
269 mass fraction (kg_w/kg_T).

270 In order to understand the structural transformations induced by the PEF pre-treatment
271 it is possible to estimate the water mass variation of each liquid phase, considering the
272 initial state as non PEF pre-treated samples and the state after the PEF pre-treatment.

273 In this sense, the next equation estimates the water mass variation after the PEF:

274
$$\Delta M_w^j = \frac{M_1 x_{w1}^j - M_0 x_{w0}^j}{M_0} \quad (2)$$

275 Where M represents the mass (g), x the mass fraction (kg/kg), the subscripts w
276 represents the water, 0 and 1 represent the samples before and after the pre-treatment
277 by PEF (V/cm) respectively, and the superscript j corresponds to a specific group of
278 molecules (ELP, ILP, ADS or overall).

279 Figure 2a shows the water mass variation in the intracellular space and in the
280 extracellular space after the PEF treatment, where it is possible to observe how the
281 water mass variation of intracellular space decreases proportionally to the increase of
282 the water mass variation of extracellular space when the electric field grows.
283 Considering that the composition of both phases is different, since the relaxation times
284 are different, the only possible explanation for this liquid phase exchange is that the
285 electric field induces a process of plasmolysis. In interphase cells, plasmolysis (which
286 is the disruption of the cell wall—plasma membrane—cortical cytoskeleton
287 continuum) is expected to exert the strongest impact on cortical microtubules since
288 they are closely linked to the plasma membrane (Ambrose, Allard, Cytrynbaum &
289 Wasteneys, 2011). These microtubules are formed by different microfilaments, and
290 one of the most important microfilament is the actin (Wen & Janmey, 2011). Actin
291 microfilament links the microtubules with the membrane by using Ca²⁺, maintaining
292 the membrane mechanical integrity (Lang et al., 2014). Therefore, any perturbation in
293 the calcium bonding between microtubules and membrane can initiate a plasmolysis
294 process.

295 Figure 2b shows how the overall water mass variation, induced by the electric field
296 applied (Traffano-Schiffo et al., 2016) is smaller (external transport) than the water
297 mass variation of internal and external liquid phase (internal transport). Moreover,

298 Figure 2b shows the water adsorbed mass variation, where the greater the electric field
299 applied the greater the amount of adsorbed water.

300

301 In order to understand the behaviors involved in the increasing of water adsorption,
302 the internal surface of samples (m²) where estimated as follows (Farroni, 2011;
303 Condon, 2006):

$$304 \quad S_i = \frac{\pi r_w^2 M (1 - x_w) X_{w0}^{ADS} N_A}{M_w} \quad (3)$$

305 Where r_w is the radius of the water molecule based in Lewis model ($1.375 \cdot 10^{-10}$ m)
306 (Pierotti, 1965), M corresponds to the mass of the sample (g), x_w is the moisture of the
307 sample (g_w/g_T), X_{w0}^{ADS} represents the moisture of the monomolecular layer obtained by
308 BET model (g_w/g_{dm}), N_A corresponds to the Avogadro constant ($6.022 \cdot 10^{23}$
309 molecules/mol) and M_w is the molecular weight of water (18 g/mol).

310 Figure 3a shows the internal surface variation of the samples according to the intensity
311 of the applied PEF pre-treatment, where at higher intensities of the electric pulses, the
312 internal surface of the sample increases. The internal surface, calculated from the
313 moisture of the monomolecular layer (equation 3), covers the entire surface with
314 capacity to adsorb water. In this sense, any process of surface release or surface
315 availability will cause an increase in the amount of adsorbed water, previously
316 observed by Traffano-Schiffo et al., 2017. As described above, the electric field
317 applied on the tissue produces a partial plasmolysis associated with the displacement
318 of calcium ions in the fixations of the actin microfilaments (cell wall-plasma
319 membrane bond). It induces a water transport from inside to the outside of the cells
320 and increases the availability of surface, as Figure 3a shows, and as was corroborated

321 in Figure 3b in which the mass of adsorbed water increases proportionally to the
322 internal surface.

323

324 In order to understand the movement of water across the kiwifruit tissue affected by
325 the PEF pre-treatment throughout OD treatment, the water mass flow was estimated
326 as follows:

$$327 \quad m_w^j = \frac{M^t x_{wi}^t - M^0 x_{wi}^0}{t} \quad (4)$$

328 Where m_w^j represents the water mass flow (g_w/s), M represents the mass sample (g),
329 x_w the water mass fraction of specific phase (g_w/g_T), t is treatment time (s), the
330 superscript j corresponds to a specific water phase (ELP, ILP or **total**), t to the treatment
331 time and 0 to the initial time.

332

333 Figure 4 shows schematically the directions that water flows can take inside the fruit
334 tissue. The water mass flow produced in the ILP can only leave, and it can be produced
335 towards the external liquid phase or towards the osmotic solution through the
336 symplastic pathways, whereas the water mass flow in the ELP can be coming in from
337 the ILP or can be leaving to the osmotic solution. **Finally, total water mass flow**
338 **represents the water molecules that cross the interface sample/osmotic solution.**

339 Water mass flow from ILP, ELP and **whole tissue (total)** was estimated by using
340 equation 4, where positive value of water mass flow represents a water flux coming in
341 the phase and negative value represents a water flux leaving the phase. Samples pre-
342 treated with PEF show an increment of ELP as Figure 4 shows, induced by a
343 plasmolysis process.

344 Figure 5 shows the evolution of each water mass flow (ILP, ELP and total) throughout
345 the OD treatment per PEF pre-treatment. As it can be appreciated, the water mass flow
346 in ELP shows positive values in non pre-treated samples (Figure 5a). Taking into
347 account that the water activity in the osmotic solution is lower than in the ELP, the
348 mass of water has to come from the ILP (as Figure 4 shows). However, negative values
349 of water mass flow in samples pre-treated (Figure 5 b, c and d) indicate that the water
350 leaves from ELP to the osmotic solution. With regard to ILP, the water mass flow
351 decreases the higher the applied PEF. Nevertheless, the overall water mass flow
352 increases the higher the applied PEF, because water from the ELP is joined with the
353 water from the ILP. Finally, the water mass flow of the ELP increases with PEF pre-
354 treatment with negative values (negative values mean that the water mass flow is
355 leaving the liquid phase), therefore only the non-pretreated samples show the effect of
356 plasmolysis. In conclusion, PEF treatment produces a partial plasmolysis in
357 parenchymatic kiwifruit tissue, and this plasmolysis process depends on the intensity
358 of PEF pre-treatment (as was observed in Figure 2).

359 **4. Conclusions**

360 It has been proven that the application of an electric field prior to the osmotic
361 dehydration produces a process of plasmolysis proportional to the applied electric
362 field. The induction of the plasmolysis process is caused by the elimination of mobile
363 charges of the medium, such as electrolytes, organic acids, etc.; among them Ca^{+2} is
364 the major culprit because it is not available to fix some of the junctions of the
365 microtubules between the cell wall and the membrane.

366 In addition, the process of plasmolysis induced by the electric field changes the
367 behavior of kiwifruit tissue during the OD process. In a normal OD, the main transport

368 is the symplastic, whereas if previously treated with PEF, the apoplastic transport is as
369 important as the symplastic, considerably increasing the rate of dehydration.

370

371 **5. Acknowledgements**

372 The authors Urszula Tylewicz and Marco Dalla Rosa want to thank for the financial
373 support provided by funding bodies within the FP7 ERA-Net CORE Organic Plus, and
374 with cofounds from the European Commission. The author Maria Victoria Traffano
375 Schiffo wants to thank the FPI Predoctoral Program of the Universidad Politécnica de
376 Valencia for support her PhD studies, ERASMUS PRÁCTICAS program to finance
377 her mobility to Italy. The authors Pedro J. Fito, Marta Castro-Giraldez and M. Victoria
378 Traffano-Schiffo acknowledge the financial support from the Spanish Ministerio de
379 Economía, Industria y Competitividad, Programa Estatal de I+D+i orientada a los
380 Retos de la Sociedad AGL2016-80643-R, **Agencia Estatal de Investigación (AEI) and**
381 **Fondo Europeo de Desarrollo Regional (FEDER).**

382

383 **6. References**

384 Agre, P., King, L. S., Yasui, M., Guggino, W. B., Ottersen, O. P., Fujiyoshi, Y., ... &
385 Nielsen, S. (2002). Aquaporin water channels—from atomic structure to clinical
386 medicine. *The Journal of Physiology*, 542(1), 3-16.

387 Ambrose, C., Allard, J. F., Cytrynbaum, E. N., & Wasteneys, G. O. (2011). A CLASP-
388 modulated cell edge barrier mechanism drives cell-wide cortical microtubule
389 organization in Arabidopsis. *Nature Communications*, 2, 430.

390 Ampomah-Dwamena, C., McGhie, T., Wibisono, R., Montefiori, M., Hellens, R. P.,
391 & Allan, A. C. (2009). The kiwifruit lycopene beta-cyclase plays a significant role in
392 carotenoid accumulation in fruit. *Journal of Experimental Botany*, 60(13), 3765-3779.

393 AOAC. (2000). AOAC, Association of Official Analytical Chemist Official Methods
394 of Analysis. Washington, D.C.

395 Baier, A. K., Bußler, S., & Knorr, D. (2015). Potential of high isostatic pressure and
396 pulsed electric fields to improve mass transport in pea tissue. *Food Research
397 International*, 76, 66-73.

398 Barba, F. J., Parniakov, O., Pereira, S. A., Wiktor, A., Grimi, N., Boussetta, N.,
399 Saraiva, J. A., Raso, J., Martin-Belloso, O., Witrowa-Rajchert, D., Lebovka, N., &
400 Lebovka, N. (2015). Current applications and new opportunities for the use of pulsed
401 electric fields in food science and industry. *Food Research International*, 77, 773-798.

402 Barboni, T., Cannac, M., & Chiaramonti, N. (2010). Effect of cold storage and ozone
403 treatment on physicochemical parameters, soluble sugars and organic acids in
404 *Actinidia deliciosa*. *Food Chemistry*, 121(4), 946-951.

405 Bezanilla, F. (2008). How membrane proteins sense voltage. *Nature Reviews
406 Molecular Cell Biology*, 9(4), 323-332.

407 Bohn, T., Walczyk, T., Leisibach, S., & Hurrell, R. F. (2004). Chlorophyll-bound
408 Magnesium in Commonly Consumed Vegetables and Fruits: Relevance to Magnesium
409 Nutrition. *Journal of Food Science*, 69(9), S347-S350.

410 Borgia, G. C., Brown, R. J. S., & Fantazzini, P. (1998). Uniform-penalty inversion of
411 multiexponential decay data. *Journal of Magnetic Resonance*, 132(1), 65-77.

412 Cano, M. P., & Marin, M. A. (1992). Pigment composition and color of frozen and
413 canned kiwi fruit slices. *Journal of Agricultural and Food Chemistry*, 40(11), 2141-
414 2146.

415 Cassano, A., Donato, L., Conidi, C., & Drioli, E. (2008). Recovery of bioactive
416 compounds in kiwifruit juice by ultrafiltration. *Innovative Food Science & Emerging*
417 *Technologies*, 9(4), 556-562.

418 Castaldo, D., Lo Voi, A., Trifiro, A., & Gherardi, S. (1992). Composition of Italian
419 kiwi (*Actinidia chinensis*) puree. *Journal of Agricultural and Food Chemistry*, 40(4),
420 594-598.

421 Castro-Giráldez, M., Fito, P. J., Dalla Rosa, M., & Fito, P. (2011). Application of
422 microwaves dielectric spectroscopy for controlling osmotic dehydration of kiwifruit
423 (*Actinidia deliciosa cv Hayward*). *Innovative Food Science & Emerging Technologies*,
424 12(4), 623-627.

425 Castro-Giráldez, M., Tylewicz, U., Fito, P. J., Dalla Rosa, M., & Fito, P. (2011).
426 Analysis of chemical and structural changes in kiwifruit (*Actinidia deliciosa cv*
427 *Hayward*) through the osmotic dehydration. *Journal of Food Engineering*, 105(4),
428 599-608.

429 Condon, J. B. (2006). *Surface area and porosity determinations by physisorption:*
430 *measurements and theory*. (1st ed.) Amsterdam, The Netherlands: Elsevier.

431 Dellarosa, N., Ragni, L., Laghi, L., Tylewicz, U., Rocculi, P., & Dalla Rosa, M. (2016).
432 Time domain nuclear magnetic resonance to monitor mass transfer mechanisms in
433 apple tissue promoted by osmotic dehydration combined with pulsed electric fields.
434 *Innovative Food Science & Emerging Technologies*, 37, 345-351.

435 Dermesonlouoglou, E., Zachariou, I., Andreou, V., & Taoukis, P. S. (2016). Effect of
436 pulsed electric fields on mass transfer and quality of osmotically dehydrated kiwifruit.
437 *Food and Bioproducts Processing*, 100, 535-544.

438 Dorai, M., Papadopoulos, A., & Gosselin, A. (2001). Influence of electric conductivity
439 management on greenhouse tomato yield and fruit quality. *Agronomie*, 21(4), 367-383.

440 Famiani, F., Battistelli, A., Moscatello, S., Cruz-Castillo, J. G., & Walker, R. P. (2015).
441 The organic acids that are accumulated in the flesh of fruits: occurrence, metabolism
442 and factors affecting their contents—a review. *Revista Chapingo Serie Horticultura*,
443 21(2).

444 Farroni, A. E. (2011). Transformaciones estructurales y físico-químicas de maíces
445 argentinos en la producción de alimentos obtenidos por procesos de gelatinización-
446 laminación (Doctoral dissertation, Facultad de Ciencias Exactas y Naturales.
447 Universidad de Buenos Aires).

448 Gürsul, I., Gueven, A., Grohmann, A., & Knorr, D. (2016). Pulsed electric fields on
449 phenylalanine ammonia lyase activity of tomato cell culture. *Journal of Food*
450 *Engineering*, 188, 66-76.

451 Havaux, M. (1998). Carotenoids as membrane stabilizers in chloroplasts. *Trends in*
452 *Plant Science*, 3(4), 147-151.

453 Johansson, I., Karlsson, M., Johanson, U., Larsson, C., & Kjellbom, P. (2000). The
454 role of aquaporins in cellular and whole plant water balance. *Biochimica et Biophysica*
455 *Acta (BBA)-Biomembranes*, 1465(1), 324-342.

456 Keutgen, A. J., & Pawelzik, E. (2008). Contribution of amino acids to strawberry fruit
457 quality and their relevance as stress indicators under NaCl salinity. *Food Chemistry*,
458 111(3), 642-647.

459 Khan, S. A., Beekwilder, J., Schaart, J. G., Mumm, R., Soriano, J. M., Jacobsen, E., &
460 Schouten, H. J. (2013). Differences in acidity of apples are probably mainly caused by
461 a malic acid transporter gene on LG16. *Tree Genetics & Genomes*, 9(2), 475-487.

462 Khin, M. M., Zhou, W., & Perera, C. O. (2006). A study of the mass transfer in osmotic
463 dehydration of coated potato cubes. *Journal of Food Engineering*, 77(1), 84-95.

464 Lang, I., Barton, D. A., & Overall, R. L. (2004). Membrane-wall attachments in
465 plasmolysed plant cells. *Protoplasma*, 224(3-4), 231-243.

466 Lang, I., Sassmann, S., Schmidt, B., & Komis, G. (2014). Plasmolysis: Loss of Turgor
467 and Beyond. *Plants*, 3(4), 583-593.

468 Ma, T., Sun, X., Zhao, J., You, Y., Lei, Y., Gao, G., & Zhan, J. (2017). Nutrient
469 compositions and antioxidant capacity of kiwifruit (*Actinidia*) and their relationship
470 with flesh color and commercial value. *Food Chemistry*, 218, 294-304.

471 Marcotte, M., Toupin, C. J., & Le Maguer, M. (1991). Mass transfer in cellular tissues.
472 Part I: The mathematical model. *Journal of Food Engineering*, 13(3), 199-220.

473 Marsh, K. B., Boldingh, H. L., Shilton, R. S., & Laing, W. A. (2009). Changes in
474 quinic acid metabolism during fruit development in three kiwifruit species. *Functional*
475 *Plant Biology*, 36(5), 463-470.

476 Maurel, C., & Chrispeels, M. J. (2001). Aquaporins. A molecular entry into plant water
477 relations. *Plant Physiology*, 125(1), 135-138.

478 Meiboom, S., & Gill, D. (1958). Modified spin-echo method for measuring nuclear
479 relaxation times. *Review of Scientific Instruments*, 29(8), 688-691.

480 Montefiori, M., McGhie, T. K., Costa, G., & Ferguson, A. R. (2005). Pigments in the
481 fruit of red-fleshed kiwifruit (*Actinidia chinensis* and *Actinidia deliciosa*). *Journal of*
482 *Agricultural and Food Chemistry*, 53(24), 9526-9530.

483 Moraga, M. J., Moraga, G., Fito, P. J., & Martínez-Navarrete, N. (2009). Effect of
484 vacuum impregnation with calcium lactate on the osmotic dehydration kinetics and
485 quality of osmodehydrated grapefruit. *Journal of Food Engineering*, 90(3), 372-379.

486 Muller, A. C. A., Scrivener, K. L., Gajewicz, A. M., & McDonald, P. J. (2013). Use
487 of bench-top NMR to measure the density, composition and desorption isotherm of C–
488 S–H in cement paste. *Microporous and Mesoporous Materials*, 178, 99-103.

489 Nakashima Y. (2001) Pulsed field gradient proton NMR study of the self-diffusion of
490 H₂O in montmorillonite gel: Effects of temperature and water fraction. *American*
491 *Mineralogist*, 86, 132–138.

492 Nishiyama, I., Fukuda, T., Shimohashi, A., & Oota, T. (2008). Sugar and organic acid
493 composition in the fruit juice of different Actinidia varieties. *Food Science and*
494 *Technology Research*, 14(1), 67-73.

495 Park, Y. S., Ham, K. S., Park, Y. K., Leontowicz, H., Leontowicz, M., Namieśnik, J.,
496 **Katrich, E.**, & Gorinstein, S. (2016). The effects of treatment on quality parameters of
497 smoothie-type 'Hayward' kiwi fruit beverages. *Food Control*, 70, 221-228.

498 Park, Y. S., Im, M. H., Ham, K. S., Kang, S. G., Park, Y. K., Namiesnik, J.,
499 **Leontowicz, H., Leontowicz, M., Katrich, E.**, & Gorinstein, S. (2013). Nutritional and
500 pharmaceutical properties of bioactive compounds in organic and conventional
501 growing kiwifruit. *Plant Foods for Human Nutrition*, 68(1), 57-64.

502 Park, Y. S., Leontowicz, H., Leontowicz, M., Namiesnik, J., Suhaj, M., Cvikrová, M.,
503 **Martincová, O., Weisz, M.**, & Gorinstein, S. (2011). Comparison of the contents of
504 bioactive compounds and the level of antioxidant activity in different kiwifruit
505 cultivars. *Journal of Food Composition and Analysis*, 24(7), 963-970.

506 Pierotti, R. A. (1965). Aqueous Solutions of Nonpolar Gases1. *The Journal of Physical*
507 *Chemistry*, 69(1), 281-288.

508 Santagapita, P., Laghi, L., Panarese, V., Tylewicz, U., Rocculi, P., & Dalla Rosa, M.
509 (2013). Modification of transverse NMR relaxation times and water diffusion

510 coefficients of kiwifruit pericarp tissue subjected to osmotic dehydration. *Food and*
511 *Bioprocess Technology*, 6(6), 1434-1443.

512 Seguí, L., Fito, P. J., & Fito, P. (2012). Understanding osmotic dehydration of tissue
513 structured foods by means of a cellular approach. *Journal of Food Engineering*,
514 110(2), 240-247.

515 Sivakumaran, S., Huffman, L., Sivakumaran, S., & Drummond, L. (2016). The
516 nutritional composition of Zespri® SunGold Kiwifruit and Zespri® Sweet Green
517 Kiwifruit. *Food Chemistry*. <http://dx.doi.org/10.1016/j.foodchem.2016.08.118>

518 Snowden, C. J., Thomas, B., Baxter, C. J., Smith, J. A. C., & Sweetlove, L. J. (2015).
519 A tonoplast Glu/Asp/GABA exchanger that affects tomato fruit amino acid
520 composition. *The Plant Journal*, 81(5), 651-660.

521 Tarchevsky I.A., Marchenko G.N. (1991). *Cellulose: Biosynthesis and Structure*.
522 Berlin, Germany: Springer-Verlag, Berlin Heidelberg, (Chapters 1 & 8).

523 Traffano-Schiffo, M. V., Laghi, L., Castro-Giraldez, M., Tylewicz, U., Roculi, P.,
524 Ragni, L., Dalla Rosa, M., & Fito, P. J. (2017). Osmotic dehydration of organic
525 kiwifruit pre-treated by pulsed electric fields and monitored by NMR. *Food Chemistry*.
526 <http://dx.doi.org/10.1016/j.foodchem.2017.02.046>

527 Traffano-Schiffo, M. V., Tylewicz, U., Castro-Giraldez, M., Fito, P. J., Ragni, L., &
528 Dalla Rosa, M. (2016). Effect of pulsed electric fields pre-treatment on mass transport
529 during the osmotic dehydration of organic kiwifruit. *Innovative Food Science &*
530 *Emerging Technologies*, 38, 243-251.

531 Tylewicz, U., Fito, P. J., Castro-Giráldez, M., Fito, P., & Dalla Rosa, M. (2011).
532 Analysis of kiwifruit osmodehydration process by systematic approach systems.
533 *Journal of Food Engineering*, 104(3), 438-444.

534 Wen, Q., & Janmey, P. A. (2011). Polymer physics of the cytoskeleton. *Current*
535 *Opinion in Solid State and Materials Science*, 15(5), 177-182.

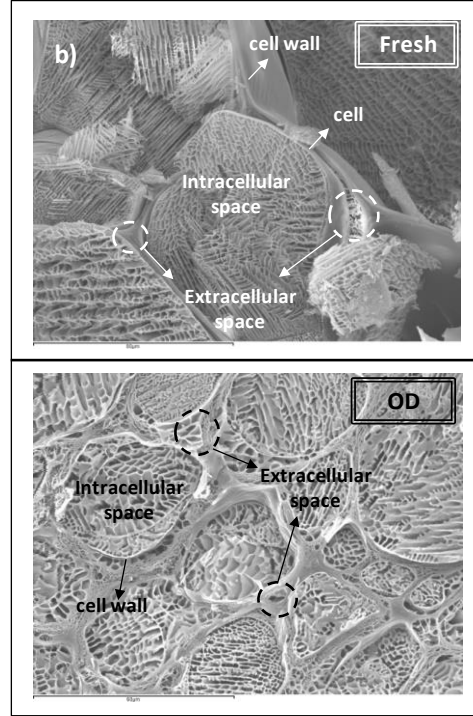
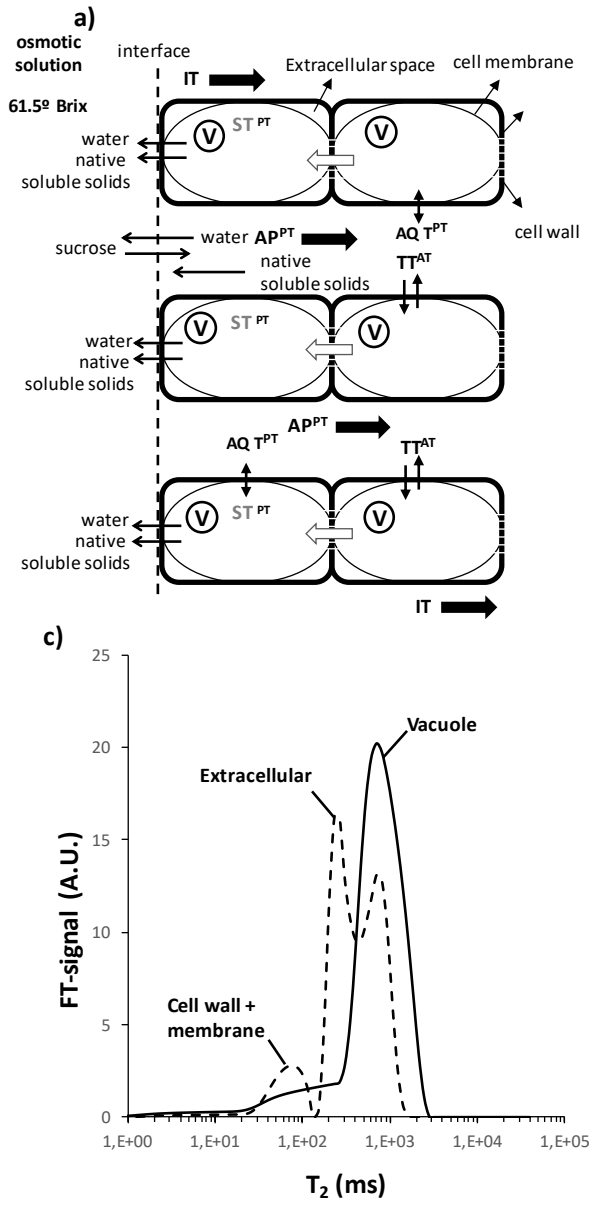


Figure 1.

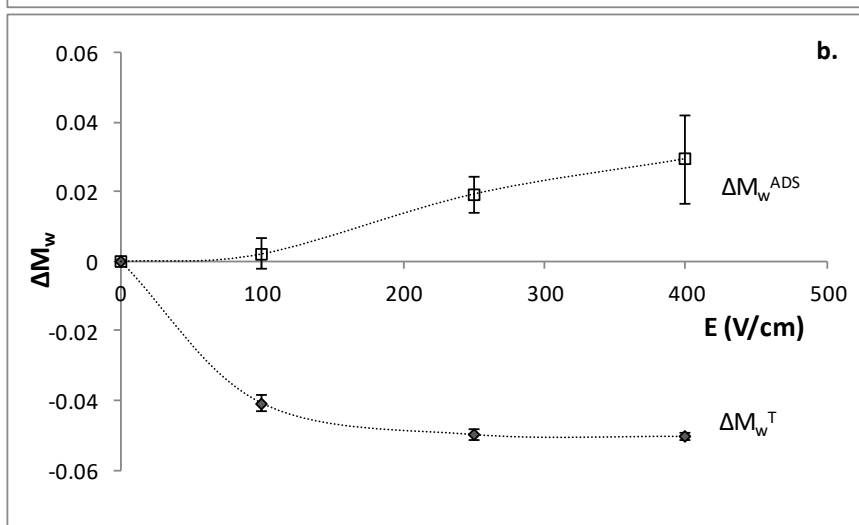
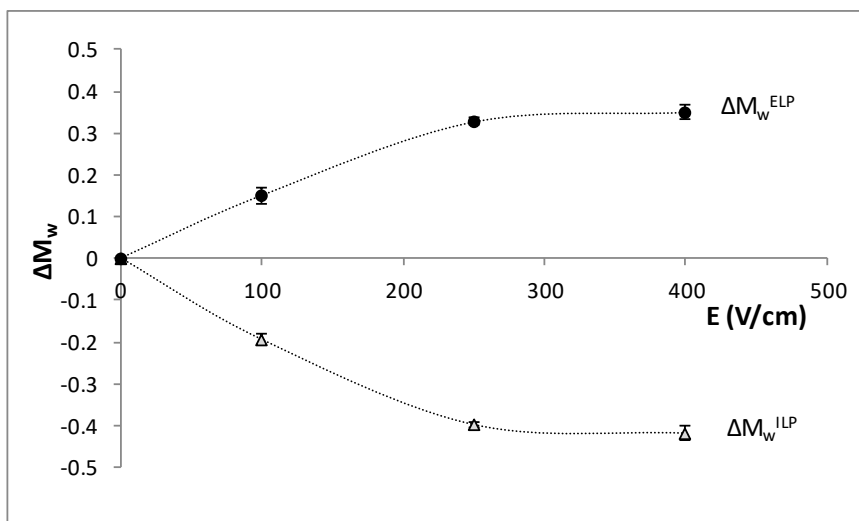


Figure 2.

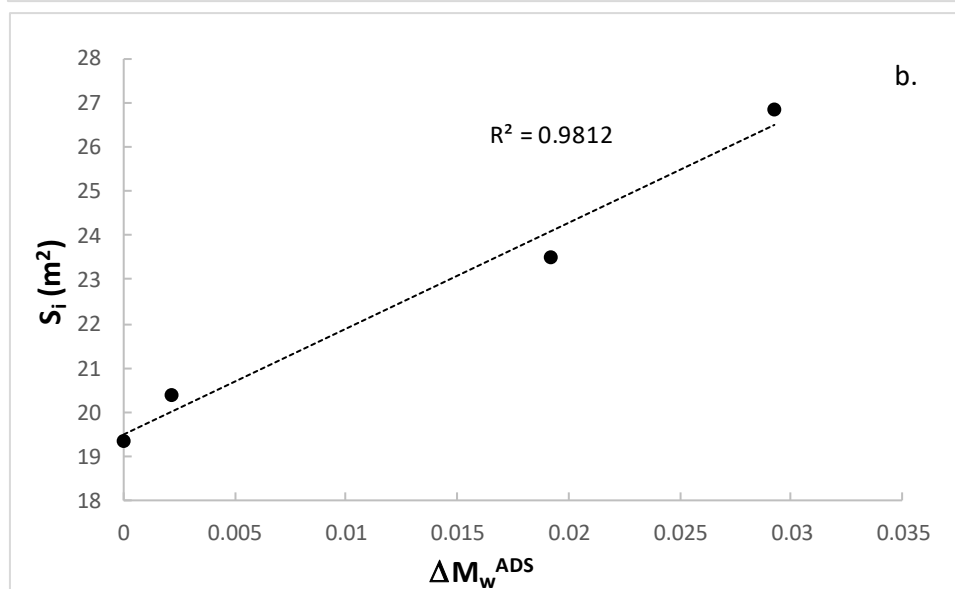
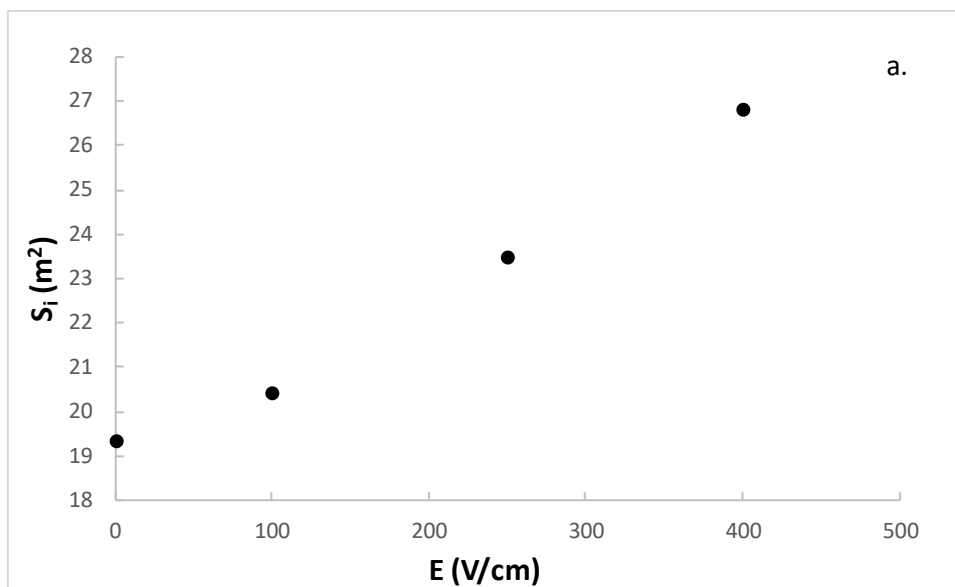


Figure 3.

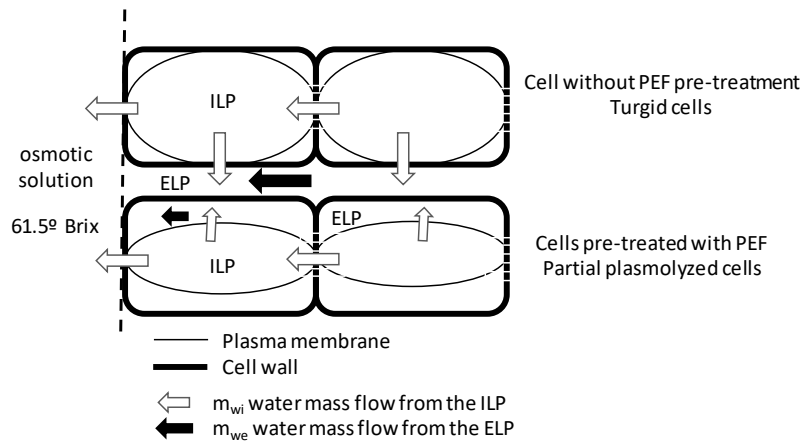


Figure 4.

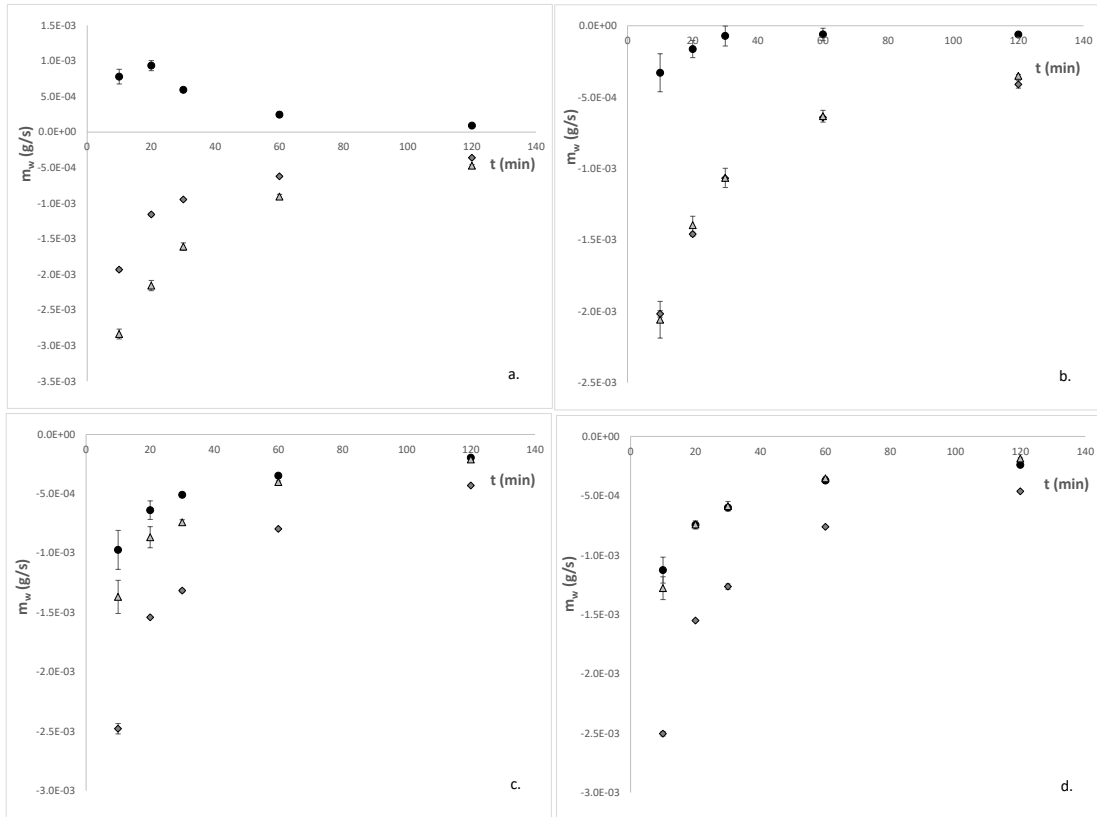


Figure 5.

Table 1. Main chemical species of fruit tissue that can be affected by the PEF.

Chemical group	Specie	Biological activity	Position	Macroscopic changes	Reference
Electrolytes	K ⁺	Secondary signal, active transmembrane pump	Intracellular, Extracellular liquid phase and membrane	Nutritional	Traffano-Schiffo et al., 2016 Sivakumaran, Huffman, Sivakumaran, & Drummond, 2016 Park et al., 2011 Bohn, Walczyk, Leisibach & Hurrell, 2004 Tarchevsky & Marchenko, 1991 Lang et al., 2014
	Na ⁺				
	Mg ²⁺	Part of the chlorophyll complex		Textural and nutritional Functional activity	
	Ca ²⁺	Calcium bridges in the middle lamella Bridges in microtubules (actin microfilaments)			
Aminoacids	Arg	Protein channel Products of the metabolic γ -aminobutyrate conversion Microtubules in cell structure	Free, cell membrane and tonoplast	Maillard browning, nutritional value and taste	Ma et al., 2017; Snowden, Thomas, Baxter, Smith, & Sweetlove, 2015; Keutgen, & Pawelzik, 2008; Castaldo et al., 1992
	Asp				
	Glu				
Chlorophylls	Chlorophyll a	O ₂ transporter, main role in photosynthesis	Liquid phase and Chloroplast	Color, functional activity	Park et al., 2013; Park et a., 2016; Montefiori McGhie, Costa, & Ferguson, 2005; Cano & Marin, 1992
	Chlorophyll b				
Carotenoids	Neolutein	Secondary role in photosynthesis	Chloroplast and chromoplast	Color, chloroplast membrane stabilizer, source of vitamin A, antioxidant capacity	Park et al., 2013; Havaux, 1998; Ampomah-Dwamena et al., 2009; Cano & Marin, 1992; Dorai, Papadopoulos, & Gosselin, 2001
	β -carotene				
Organic acids	Citric acid	Krebs cycle intermediate; part of cytosolic pyruvate metabolism	Extra and Intracellular liquid phases	Antioxidant	Sivakumaran et al., 2016; Famiani, Battistelli, Moscatello, Cruz-Castillo, & Walker, 2015 Khan et al., 2013; Nishiyama, Fukuda, Shimohashi, & Oota, 2008 Marsh, Boldingh, Shilton, & Laing, 2009 Barboni, Cannac, & Chiramonti, 2010; Cassano, Donato, Conidi, & Drioli, 2008
	Malic acid			Acidity, flavor	
	Quinic acid	Fruit maturity		Sugar/acid balance, flavor	
	Ascorbic acid	Antioxidant, enzyme Cofactor, electron transport, chloroplast activity		Bioactive compound	

Table 2. Intensity values of the samples obtained by TD-NMR during OD treatment

(I^{ADS} : intensity of water adsorbed; I^{ELP} : intensity of extracellular liquid phase; I^{ILP} : intensity of internal liquid phase).

E (V/cm)		OD time (min)					
		0	10	20	30	60	120
0	I^{ADS}	31 ± 4	41.78 ± 0.91	45 ± 2	50 ± 8	59 ± 2	74 ± 2
	I^{ELP}	25 ± 8	58 ± 5	103 ± 6	132 ± 5	120 ± 9	131 ± 11
	I^{ILP}	251 ± 4	183 ± 12	165 ± 9	125 ± 11	124 ± 12	107 ± 7
100	I^{ADS}	33 ± 2	49 ± 3	59 ± 1	61 ± 3	73 ± 5	77 ± 5
	I^{ELP}	91 ± 7	101 ± 12	115 ± 8	126 ± 11	126 ± 14	123 ± 6
	I^{ILP}	208 ± 7	172 ± 13	146 ± 7	131 ± 13	96 ± 8	104 ± 8
250	I^{ADS}	39 ± 2	48 ± 2	56 ± 3	54 ± 6	57 ± 4	70 ± 12
	I^{ELP}	163 ± 5	175 ± 9	174 ± 9	184 ± 5	165 ± 10	169 ± 6
	I^{ILP}	125 ± 2	101 ± 7	91 ± 10	71 ± 8	70 ± 2	57 ± 8
400	I^{ADS}	39 ± 3	50.8 ± 0.4	53 ± 6	54 ± 5	64 ± 2	60 ± 6
	I^{ELP}	167 ± 4	183 ± 9	174 ± 9	183 ± 6	181 ± 2	170 ± 5
	I^{ILP}	107 ± 14	86 ± 5	79 ± 8	75 ± 7	61 ± 6	68 ± 7

RESEARCH HIGHLIGHTS

- The application of PEF as OD pre-treatment removes the mobile charges of the tissue.
- PEF pre-treatment produces a greater plasmolysis, the greater the electric field applied.
- In samples pre-treated with PEF, calcium is the major culprit of the plasmolysis.
- PEF pre-treatment affects the normal behavior of the internal transports.
- After PEF, apoplastic transport is as important as the symplastic.

Industrial relevance

This research describes the effect of the PEF pre-treatment of osmotic dehydration in the microstructure and in the internal water liquid phases transports of the kiwifruit tissue by using TD-NMR. The results of this research have demonstrated that the application of an electric field prior to the osmotic dehydration produces a process of plasmolysis more the greater the electric field applied, due to the elimination of the mobile charges of the medium and mainly affecting the internal transports. Therefore, PEF pre-treatment accelerate the OD treatment preserving the structure and consequently remaining the life cycles, necessities to obtain a long shelf life of the product. It has been demonstrated the useful of the TD-NMR as a technique able to analyzed the effect of PEF at a microstructural degree.

FIGURE CAPTIONS

Figure 1. a) Schematic representation of system and the cellular transports during osmotic dehydration treatment (adapted from Traffano-Schiffo et al., 2016), b) Cryo-SEM observation of fresh (750x) and 30 min osmodehydrated kiwifruit tissue (1000x), c) T_2 -weighted signal distribution, normalized to unitary area, registered on fresh samples treated by PEF at 0 (black solid line) and 250 V/cm (black dashed line) samples before OD treatment (adapted from Traffano-Schiffo et al., 2017). PT: Passive transport, AT: Active transport, V: Vacuole, IT: Internal transport, ST: Symplastic transport, AP: Apoplastic transport, AQ T: Aquaporins transmembrane transport (water) and TT: Transmembrane transport.

Figure 2. Water mass variation a. (●) extracellular liquid phase (ELP), (▲) intracellular liquid phase (ILP) and b. (□) adsorbed water (ADS) and (◆) total mass (T) variation at different PEF treatments (V/cm).

Figure 3. a. Internal Surface of the solid matrix; b. relationship between the water mass variation of the adsorbed water and the internal surface of the solid matrix.

Figure 4. Schematic representation of cell structure with and without PEF pre-treatment.

Figure 5. Water mass flow during osmotic dehydration treatment of the samples pre-treated with PEF. a. 0 V/cm, b. 100 V/cm, c. 250 V/cm and d. 400 V/cm, where: (●) extracellular liquid phase (ELP), (▲) intracellular liquid phase (ILP) and (◆) total water mass flow.

